The *Gdac1* locus modifies spontaneous and Salmonella-induced colitis in mice deficient in either *Gpx2* or *Gpx1* genes

R. Steven Esworthy[1], **Byung-Wook Kim**[1], **Yufeng Wang**[2], **Qiang Gao**[2], **James H Doroshow**[3], **Thomas L Leto**[4], and **Fong-Fong Chu**[1,5]

[1]Department of Radiation Biology, Beckman Research Institute of City of Hope, Duarte, CA 91010

[2]Department of Gastroenterology and Hepatology, The First Affiliated Hospital, Henan University of Science and Technology, Luoyang, Henan, China, 471000

[3]National Cancer Institute, Bethesda, MD 20816

[4]Laboratory of Host Defenses, National Institute of Allergy and Infectious Diseases, NIH, Rockville, MD 20852

Abstract

We previously identified a *Gdac1* (Gpx-deficiency-associated colitis 1) locus that influences the severity of spontaneous colitis in Gpx1- and Gpx2-double knockout (Gpx1/2-DKO) mice. Congenic Gpx1/2-DKO mice in the129S1/SvImJ (129) background but carrying the *Gdac1^B6* allele have milder spontaneous colitis than 129 Gpx1/2-DKO mice carrying the *Gdac1^129* allele. Here, we evaluated the effect of the *Gdac1^B6* allele on 129 strain non-DKO mice that had a wild-type (WT) *Gpx1* or *Gpx2* allele and WT mice. We found the congenic *Gdac1^B6* Gpx2-KO, Gpx1-KO and WT mice also had better health than the corresponding 129 mice measured by at least one of the parameters including disease signs, colon length or weight gain. The *Gdac1^B6* allele prevented loss of goblet cells and crypt epithelium exfoliation in the Gpx1/2-DKO mice, but did not affect epithelial cell apoptosis or proliferation. Because *Gdac1^B6* affects gut dysbiosis in the DKO mice, we then tested its impact on bacteria-induced colitis in non-DKO mice. First, we found both Gpx1-KO and Gpx2-KO mice were susceptible to *Salmonella enterica serotype* Typhimurium (*S.* Tm)-induced colitis under conditions where WT B6 and 129 mice were resistant. Second, the *S.* Tm-infected *Gdac1^B6* Gpx1-KO mice had stronger inflammatory responses than 129 Gpx1-KO, 129 Gpx2-KO with both Gdac1 allele and WT mice by having higher mRNA levels of Nod2, Nox2, Tnf and Cox2. We conclude that the *Gdac1* locus affects both spontaneous and *S.* Tm-induced colitis in 129 non-DKO mice although in opposite directions.

Keywords

[5]Correspondance: Fong-Fong Chu, Department of Radiation Biology, Beckman Research Institute of City of Hope, 1500 Duarte Road, Duarte, CA 91010-3000, fchu@coh.org, Tel: 626-256-HOPE x63831, Fax: 626-930-5330.

INTRODUCTION

Mice deficient for selenium-dependent glutathione peroxidases (GPX) 1 and 2 have large variation in the penetrance and severity of colitis depending on their genetic background. Gpx1/2-double knockout (DKO) mice in the C57BL/6J (B6) background have mild colitis, while DKO mice in the 129S1/SvImJ (129) background have early-onset severe colitis. We mapped a locus that contributes to this difference to distal chromosome 2 (118–125 mbp, 95% confidence interval), named the locus *glutathione peroxidase-deficiency-associated colitis 1* (*Gdac1*) and created a 129 congenic line that differs at the *Gdac1*[B6] locus [1, 2]. The *Gdac1* locus contains 128 well-annotated protein coding genes [2, 3]. This entire region and some flanking area are preserved in humans at chromosome 15q: 38–49 mbp. The human equivalent of *Gdac1* contains a human Crohn's disease locus (SNP rs16967103) with four candidate genes, including *RASGRP1* and *SPRED1*, and an ulcerative colitis locus (SNP rs28374715) that contains 11 candidate genes [2, 3]. Since only a handful of humans could be depleted of GPX1 and GPX2 to the extent found in Gpx1/2-DKO mice [4], before we can apply the knowledge gained from studying the mouse *Gdac1* locus to human colitis, we need to illustrate the *Gdac1* effect in mice without complete GPX depletion.

In studies to identify the *Gdac1* locus in Gpx1/2-DKO mice, we measured colon length, disease activity index, *E. coli* overgrowth and colon pathology score [2, 3]. Through our breeding scheme to generate DKO mice, we also produced many 129 non-DKO mice that carried one wild-type (WT) *Gpx1* or *Gpx2* allele of both *Gdac1* genotypes (129 and B6). Knowing that selenium-deficient Gpx2-KO (non-DKO) mice in a mixed B6 and 129 background also had spontaneous ileocolitis [5], we questioned here whether these 129 non-DKO mice also have significant colitis. If so, would *Gdac1* also affect spontaneous colitis in these non-DKO mice?

The *Gdac1* locus has a distinct effect on *E. coli* overgrowth in DKO mice [2, 3]. We have found that *E. coli* overgrowth in the cecum is a distinct feature of 129 DKO mice but not B6 DKO, 129 WT or 129 non-DKO mice [6]. *E. coli* overgrowth is a reliable marker for gut dysbiosis, which is linked to common human intestinal disorders, such as Crohn's disease and colorectal cancer [7]. Because commensal gut microbes also participate in defense mechanisms to fend off invading pathogens [8], we questioned whether the *Gdac1* locus affected bacteria-induced colitis.

Salmonella enteric serotype Typhimurium (*S*. Tm) is a leading cause of food poisoning in humans and causes 580 deaths annually in the United States [9, 10]. *S*. Tm has been widely used as a mouse colitis model to study strategies by which enteropathogenic bacteria break colonization resistance [11]. Alteration of gut microbiota with different antibiotics can affect mouse susceptibility to *S*. Tm infection [12]. Thus, we tested whether the *Gdac1* locus can affect *S*. Tm infection in 129 Gpx1-KO and Gpx2-KO mice, which have almost no and very mild spontaneous colitis, respectively.

Here we report that the *Gdac1* locus significantly affected spontaneous and *S*. Tm-induced colitis in Gpx1-KO mice. However, while the *Gdac1*[B6] locus attenuated spontaneous colitis, it exacerbates *S*. Tm-induced colitis. Intriguingly, 129 Gpx1-KO and Gpx2-KO mice were susceptible to *S*. Tm-induced colitis conditions that WT B6 and 129 mice were resistant. Thus, we provide the first evidence to demonstrate the function of GPx1 and GPx2 against *S*. Tm colonization and infection. This finding may explain why selenium deficiency increases the susceptibility of humans and other animals to infectious diseases [13].

Materials and Methods

Mice

The *Gpx*1/2-DKO colony was maintained in both the B6 and 129 strains [2]. Because DKO dams are poor fosters, male DKO mice were bred to Gpx1−/− Gpx2+/− (Gpx1-KO) females or Gpx1+/− Gpx2−/− (Gpx2-KO) females to generate offspring having the same genotypes as the parents. WT mice were derived from the DKO colonies by inbreeding heterozygous mice and maintained as separate colonies. We established a congenic 129 line that carried the *Gdac1*^{B6} locus. These 129-*Gdac1*^{B6} DKO mice had milder colitis than the parent 129 DKO mice [1, 2]. Mice were reared on semi-purified diets (Harland Teklad; casein, sucrose, corn oil; TD 06306 and TD 06307) designed to mimic LabDiets 5020 (10% corn oil, Purina) and 5001 (5% corn oil) for calories and macronutrients. The diets used AIN76A vitamin and micronutrient specifications. All animal studies reported here were approved by the City of Hope Institutional Animal & Use Committee.

Salmonella inoculation

A virulent strain of *S.* Tm, IR715, was obtained from Dr. Andreas J. Baumler (University of California, Davis), who derived this strain from the 14028 isolate (American Type Culture Collection)[14]. *S.* Tm was grown aerobically at 37oC in Luria-Bertani (LB) containing 50 μg/mL nalidixic acid (Sigma) and harvested after overnight growth. To allow colonization of *S.* Tm, 6- to 8-week-old mice were either pre-treated with broad-spectrum streptomycin (20 mg in 25 μL PBS per mouse) by oral gavage for one day or with anaerobe-specific metronidazole (0.75 g/L in drinking water) for four days and then gavaged with ~2×10^7 CFU of bacteria [15]. Streptomycin-treated mice were analyzed 1 and 2 days after inoculation with *S.* Tm. Metronidazole-treated mice were euthanized 4 days post-inoculation, when mice had the most consistent pathology [12]. Numbers of mice in each group are provided in figure legends. All groups are male mice, except WT B6 group has 5 females and 3 males.

Mouse pathology and phenotypes

Disease activity index (DAI). Scoring criteria for DAI were reported previously [2]. The final score was obtained by combining scores from the growth/wasting (scores 0–4) and diarrhea (scores 0–4) categories, giving scores ranging from 0 to 8. Mice with scores of 6 and above were considered morbid and were euthanized within 24 h. Some mice with scores of 5 were classified as morbid, post-hoc, based on a review of disease signs.

Colon pathology. Pathology on sections stained with hematoxylin and eosin (H&E) was scored in a blinded fashion using a 14-point system as previously described [1]. Scores of 0–6 generally reflect presence of crypt apoptosis/hyperproliferation and mucin depletion without overt signs of inflammation. For scores greater than 6, acute inflammation is generally evident together with neutrophil infiltration, gland abscesses or erosion of the epithelium [1, 6]. Scores approaching 11 reflect considerable, in some cases nearly complete erosion of the epithelium.

Quantization of goblet cells, apoptotic, mitotic cells and exfoliation. Goblet cells were counted on cross sections of mid-lower colon after staining with alcian blue and counter staining with nuclear fast red. The number of alcian blue stained cells from cross sections of colon was counted from 5–10 mice in each group as detailed in the figure legend. The mitotic and apoptotic cells as well as exfoliated cells were identified by morphology in H&E stained cross sections. The number of crypts with at least one mitotic, apoptotic figure or exfoliated cells in each cross section was divided by total number of crypt to determine fraction. Each analysis was done on 90–200 crypts from 5–10 mice. Apoptotic cells were

also analyzed with the TUNEL method to detect DNA strand breaks using ApopTag Peroxidase In Situ Apoptosis Detection Kit (Millipore). All analysis was done in a blinded fashion.

E. coli overgrowth. Cecum contents were analyzed for *E. coli* colony forming units (CFU)/gm on LB plates grown aerobically at 37°C for 18–22 h. The cecum is a disease site in the Gpx1/2-DKO mice [1, 6]. Large colonies were scored as *E. coli*, and less frequently detected small colonies were identified as *Enterococcus sp.* (*hirae, gallinarum* or *faecalis*). Colony identity was established by sequencing rDNA amplified (RISA) from single colonies of both *E. coli* and *Enterococcus sp. E. coli* colonies were also were verified by the Clinical Microbiology Laboratory at City of Hope [6]. Spot checks were performed on randomly selected large colonies throughout the project to confirm their identities. Single dilutions of cecal contents were plated with sensitivity of ~2×10^6-1×10^7 CFU/gm [1, 6]. Zero colonies were entered as a default of 1×10^6 CFU/gm, which was empirically determined to be the upper limit for healthy mice at this age [6, 16]. Salmonella CFUs were estimated similarly, using nalidixic acidcontaining LB plates. Spot checks of colonies were done using previously reported RISA primers with a standard of the original clone [6]. *Salmonella* RISA banding analyzed on 1.3% agarose gels was easily distinguishable from both *E. coli* and *Enterococcus*.

RT-PCR to evaluate gene expression

Mice were euthanized by CO_2 asphyxiation. Distal colon tissues were dissected and stored in RNAlater (Qiagen). For synthesis of cDNA, colon tissues were homogenized with a Polytron homogenizer (PT 1200E: Brinkmann Kinematica, Fisher Scientific) and sonicated. Total RNA was isolated using the RNeasy Mini kit (Qiagen). cDNA was synthesized from 2 μg total RNA by using M-MLV reverse transcriptase (Promega, Madison, WI, USA) in the presence of random hexamers (1 μg; Invitrogen). Real-time quantitative PCR (qPCR) was performed with the Eva qPCR SuperMix kit containing SYBR green dye (Biochain Institute, Hayward, CA, USA) and using an iQ5 Detection system (Bio-Rad Laboratories, Hercules, CA, USA). Data analysis was done as previously reported [2]. RNA quantity was normalized to β-actin or villin for whole tissue or epithelial-specific expression, respectively. Each assay was performed in duplicate. Primer sequences are listed in Table 1.

Statistical analysis

Comparison of different groups on the percentage of mice that showed disease signs and morbidity (Fig 1A) was done with Fisher's exact test. Comparison on colon length (Fig 1B), body weight (Fig 1C), goblet cell number (Fig 2D), fraction crypts with exfoliation, apoptosis, mitosis, (Fig 3A-C, and Sup 1B) and mRNA expression levels (Fig 5, 6, Sup Fig 3) was done with 1-way ANOVA, Tukey's multiple comparison test. Gut dysbiosis and cecum pathology scores (Fig 1D, 4A and 4B) were analyzed using Kruskal-Wallis test with Dunn's multiple comparison test. When $P<0.05$ is considered significant. All tests were done with GraphPad PRISM, version 6.01.

RESULTS

The Gdac1 locus affects spontaneous colitis in mice with and without Gpx deficiency

We previously identified the *Gdac1^B6* locus, which alleviated the severity of colitis in 129 Gpx1/2-DKO mice [1, 2]. To determine whether the effect of the *Gdac1^B6* locus can be detected in 129 mice without GPX deficiency, we evaluated five parameters indicative of colitis (disease signs, morbidity, body weight, colon length and dysbiosis) in 129 Gpx1-KO and Gpx2-KO mice that had a WT *Gpx2* or *Gpx1* allele, respectively, as well as 129 WT mice. Disease signs evaluated included weight loss and diarrhea, which were used to

determine DAI. Morbidity was defined as loss of at least 20% of peak body weight and/or exhibiting diarrhea for more than one day. Analysis of a cohort of 574 DKO, 156 *Gdac1*[B6]-DKO, 315 Gpx2-KO, 80 *Gdac1*[B6]-Gpx2-KO, 352 Gpx1-KO, 114 *Gdac1*[B6]-Gpx1-KO, 30 WT and 10 *Gdac1*[B6] WT mice, revealed that *Gdac1*[B6] significantly alleviated disease signs in DKO, Gpx2-KO and Gpx1-KO mice (Fig 1A). Analysis of a cohort of 106 DKO, 69 *Gdac1*[B6] DKO, 46 Gpx2-KO, 15 *Gdac1*[B6] Gpx2-KO, 36 Gpx1-KO, 8 *Gdac1*[B6] Gpx1-KO, 22 WT and 29 *Gdac1*[B6] WT mice, revealed that *Gdac1*[B6] mice had longer colons in DKO, Gpx1-KO and WT mice determined at 22 days of age (Fig 1B). From a cohort of 22-day-old 339 DKO, 147 *Gdac1*[B6] DKO, 193 Gpx2-KO, 72 *Gdac1*[B6] Gpx2-KO, 293 Gpx1-KO, 97 *Gdac1*[B6] Gpx1-KO, 36 WT and 43 *Gdac1*[B6] WT mice, *Gdac1*[B6] DKO and Gpx2-KO mice gained more weight than *Gdac1*[129] counterparts (Fig 1C). Therefore, the *Gdac1*[B6] locus provided better health than the *Gdac1*[129] counterparts not only in DKO, but also Gpx2-KO, Gpx1-KO and WT mice determined by at least one of the three criteria: disease signs, colon length and body weight.

Gpx2, but not Gpx1, deficiency induces mild spontaneous colitis

We had reported that selenium-deficient Gpx2-KO mice (in a mixed B6 and 129 genetic background) were prone to ileocolitis [5]. In the current study, we found the selenium-adequate 129 Gpx2-KO mice had a significantly higher incidence of disease signs and *E. coli* overgrowth (gut dysbiosis) than did 129 Gpx1-KO and WT mice (Fig 1A and 1D). The congenic *Gdac1*[B6] Gpx2-KO mice had shorter colon than congenic *Gdac1*[B6] Gpx1-KO and WT mice (Fig 1B). These results suggest that Gpx2-defiency predisposes gut to inflammation. However, Gpx1 also protects mouse gut from developing full-blown disease, which occurs in Gpx1/2-DKO mice.

The Gdac1 locus affects goblet cell depletion and exfoliation of crypt epithelium but not apoptosis and mitosis of epithelium

Goblet cell depletion is a prominent feature of Gpx1/2-DKO and IBD patients [17]. We determined whether the 129-*Gdac1*[B6] can decrease goblet cell depletion in 129 Gpx1/2-DKO mice by counting the total number of goblet cells in cross section of lower colon (Fig 2A-2C). We found the colon of 129-*Gdac1*[B6] DKO mice had significantly higher number of goblet cells than 129 DKO mice, although still lower than 129 WT mice (Fig 2D).

Other prominent pathological features of Gpx1/2-DKO mice include rampant exfoliation, proliferation and apoptosis of colon crypt epithelial cells [18]. We also investigated whether *Gdac1*[B6] can decrease these pathological features. Impressively, *Gdac1*[B6] DKO mice had dramatically lower number of exfoliated cells than 129 DKO mice, to the same level as 129 Gpx2-KO mice, while 129 Gpx1-KO and WT mice did not have any detectable crypt exfoliation (Fig 3A). Although *Gdac1*[B6] DKO mice did not have lower incidences of apoptotic and mitotic cells than 129 DKO mice (Fig 3B and 3C), the numbers of apoptotic and mitotic cells in 129 DKO mice were most likely grossly underestimated due to the severe inflammation resulting distorted morphology and restitution [1]. *Gdac1* did not affect crypt mitosis and apoptosis in WT mice. The fraction of crypts with mitosis was 0.145 analyzed from both 9 129 and 7 Gdac1[B6] WT mice, and faction of crypt apoptosis was 0.004 and 0.009, respectively (P=0.21).

129 Gpx2-KO mice also had elevated number of apoptotic cells compared to Gpx1-KO and WT mice (Fig 3B and Sup Fig 1). This result is similar to what we reported in B6 Gpx2-KO mice [19].

129 Gpx1-KO and 129 Gpx2-KO mice are more susceptible to S. Tm-induced colitis than WT B6 and 129 mice

We reported that 129 DKO, but not B6 DKO, colon had *E. coli* overgrowth, which indicated gut dysbiosis [6]. It is necessary to disrupt gut microbes with antibiotics to allow invasion of pathogenic bacteria such as *S*. Tm to induce colitis in mice [12]. Different antibiotics were able to produce different types of dysbiosis to alter susceptibility to *S*. Tm infection in a strain-dependent manner [12]. As expected, when we pretreated B6 and 129 WT mice as well as 129 Gpx1-KO and 129-Gdac1^B6 Gpx1-KO mice with streptomycin, a broad spectrum antibiotic, both strains WT mice developed acute colitis and had similar scores (data not shown).

However, when we pretreated mice with metronidazole (Met), a nitroimidazole antibiotic that is effective against anaerobes and routinely used to treat IBD, and inoculated mice with the same amount of *S*. Tm as used for streptomycin-treated mice, neither B6 nor 129 WT mice were infected by S. Tm or developed colitis (Fig 4A and 4B). Unexpectedly, Met-pretreated 129 Gpx1-KO (carrying either *Gdac1* allele) were highly susceptible to *S*. Tm-induced colitis (Fig 4). While Met-pretreated Gpx2-KO mice carrying either *Gdac1* allele do not have statistically significant higher inflammation scores than WT mice (Fig 4B), when combined, Gpx2-KO mice have significantly higher pathology than WT mice (P<0.05). The inflamed cecum from both 129 Gpx1-KO and Gpx2-KO mice had lost epithelial cells and were infiltrated with inflammatory cells (Fig 4D).

The *Gdac1^B6* allele exacerbates colitis in Gpx1-KO mice infected with *S*. Tm

Because the inflamed cecum had lost epithelial cells, we determined the levels of *villin* mRNA, which is highly expressed in differentiated epithelial cells and is associated with actin filaments [20] to quantify the extent of epithelial loss. We found that *S*. Tm-infected both 129 and congenic *Gdac1^B6* Gpx1-KO as well as *Gdac1^B6* Gpx2-KO mice had two- to four-fold lower expression of *villin* mRNA than did B6 and 129 WT mice (Fig 5A). The villin gene expression levels when normalized with β-actin are inversely correlated with pathology scores with correlation coefficient of -0.73 (Sup Fig 2). This result strongly suggests that loss of villin gene expression is due to loss of epithelial cells.

Because the inflamed cecum had many infiltrating inflammatory cells, we used the mRNA levels of genes highly, if not exclusively, expressed in inflammatory cells to quantify the extent of inflammation. We analyzed Nod2, Tnf and Nox2 gene expression, since *Nod2* is highly expressed in monocytes in submucosa [21], Tnf is mainly expressed in macrophages (RefSeq, NCBI), and Nox2 is exclusively expressed in neutrophils and monocytes [22, 23]. Because these genes are expressed in non-epithelial cells, their expression levels were normalized to β-actin mRNA levels. Contrary to the anti-inflammatory activity of *Gdac1^B6* in spontaneous colitis, these three genes were expressed at significantly higher levels in the *Gdac1^B6* Gpx1-KO mice than 129 Gpx1-KO and other types of mice (Fig 5B-5D). These results suggest that *Gdac1^B6* allele exacerbated *S*. Tm-induced colitis in Gpx1-KO mice.

The acute colitis in Gpx1-KO mice is associated with myeloid cells

Although *Salmonella*-colonized Gpx2-KO mice have a similar severity of colitis pathology and loss of epithelial cells as Gpx1-KO mice, regardless of their *Gdac1* genotype, the Gpx2-KO mice clearly had milder inflammatory responses as indicated by their low levels of expression of inflammatory genes. In addition to *Nod2*, *Tnf* and *Nox2* analyzed above, which are highly expressed in monocytes, macrophages and neutrophils, we quantified *Cd14* and *Cox2* mRNA levels. CD14 is a glycosyl-phosphatidylinositol-linked glycoprotein that functions as a co-receptor of Toll-like receptors to sense microbes, and is highly expressed on the surface of myeloid cells [24–26]. COX2 is highly expressed in the lamina propria,

and much lower in the intestinal epithelial cells [27]. *Cox-2* expression in myeloid and endothelial cells, but not in epithelial cells affects DSS-induced colitis [28]. We found *Cd14* and *Cox2* mRNA levels were highly elevated in *Gdac1*^{B6} Gpx1-KO mice (Fig 6A and 6B).

We analyzed the expression levels of three more genes, *Ifng, IL1β* and *Nlrp3*, which are highly expressed in innate immune cells. The primary source of interferon gamma (Ifng) is lymphoid cells including natural killer cells and innate lymphoid cells [29, 30]. The primary source of IL1β is macrophages, and IL1β is activated by Nlrp3 inflammasome [31]. Nlrp3 is a member of Nod-like receptor proteins containing NACHT, leucine-rich repeat and pyrin domains [32]. Nlrp3 mRNA is highly expressed in the neutrophils and myeloid cells [33]. While these genes were expressed at above background levels in Gpx1-KO mice, only IL1β and Nlrp3 expression was significantly elevated in *Gdac1*^{B6} Gpx1-KO mice compared to control mice (Sup Fig 3).

Taken together, these results strongly suggest that *Salmonella*-induced acute colitis in *Gdac1*^{B6} Gpx1-KO mice is driven by infiltrating inflammatory cells.

Induction of *Duox2* and *Gpx2* gene in S. Tm-infected Gdac1^{B6} Gpx1-KO mice

It was reported that *Salmonella enteritidis* infected rat colon had 2–3-fold higher expression of Duox2 and Gpx2 genes when normalized to *Rps26*, which encodes ribosomal protein S26 [34]. Here, we analyzed *Duox2* and *Gpx2* mRNA levels and normalized the results to villin because of their restricted epithelial expression [35] [19]. *Duox2* gene expression was elevated ~20- to 30-fold in infected 129 *Gdac1*^{B6} Gpx1-KO mice as compared to Gpx2-KO and WT mice (Fig 6D). In the infected 129 Gpx2-KO mice, the *Duox2* mRNA was elevated ~6 fold as compared to 129 WT mice. However, this difference was not statistically significant.

We also examined whether Gpx2 mRNA expression is elevated in the inflamed tissue, because we have shown that intestinal *Gpx2* is highly induced by γ irradiation [36]. Although the 4 to 5-fold elevated Gpx2 mRNA levels in 129 Gpx1-KO and *Gdac1*^{B6} Gpx1-KO mice compared to uninfected Gpx1-KO and WT mice were not statistically significant (Sup Fig 3D), when analyzing the combined infected Gpx1-KO of both *Gdac1* alleles with combined uninfected Gpx1-KO or WT mice, Gpx2 expression is significantly induced.

Because Nox1 can mediate TNF-induced apoptosis [37], and Nox1 is highly expressed in colon epithelium [38], we also analyzed Nox1 mRNA levels. Probably due to the big spread of Nox1 mRNA levels within the group, the elevated Nox1 mRNA levels in the S. Tm-infected Gpx1-KO and Gpx2-KO mouse colon did not reach statistical significance (Fig 6C).

DISCUSSION

We previously identified the *Gdac1* locus in mouse chromosome 2, which modifies the severity of colitis, by comparing the phenotypes of 129 and *Gdac1*^{B6} congenic Gpx1/2-DKO mice [1, 2]. Here, we have demonstrated that the *Gdac1* locus also affects spontaneous colitis in Gpx2-KO, Gpx1-KO mice and growth in WT mice, as assessed by signs of the disease, colon length or body weight. Thus, the *Gdac1* effect is not limited to DKO mice, but also is evident in mice without complete deficiency in GPX activity. In all cases, *Gdac1*^{B6} congenic mice were healthier and/or more robust than their 129 counterparts. These findings suggest that these congenic *Gdac1* mice can be used as a mouse model to study the candidate genes of two human disease loci: a Crohn's disease locus (comprising 4 genes, including *RASGRP1* and *SPRED1*) and an ulcerative colitis locus (comprising 11

genes). Both of these loci map to human chromosome 15 in the area corresponding to the mouse *Gdac1* locus [2, 3].

We have shown that gut dysbiosis manifested as *E. coli* overgrowth can be detected in 129 DKO but not B6 DKO or 129 WT mice [6]. Here, we showed that the *Gdac1* locus affected gut dysbiosis in 129 DKO and Gpx2-KO mice. Because antibiotic-induced dysbiosis allows colonization of bacterial pathogens such as *Salmonella enterica serovar* Typhimurium (S. Tm) to cause colitis in a mouse strain-dependent manner [12], we explored whether the *Gdac1* locus affected S. Tm infection. In contrast to its effect on spontaneous colitis, the *Gdac1*[B6] locus exacerbates bacteria-induced colitis in Gpx1-KO mice. This is in partial agreement with the report that Met-treated 129 WT mice were resistant to S. Tm, while Met-treated B6 WT mice were sensitive [12] since we found both Met-treated B6 and 129 WT mice were resistant to S. Tm infection. The different outcome is due to a slightly different procedure used; we used a shorter metronidazole pretreatment (4 days vs. 7 days) as well as a 13.5-fold lower dose (2×10^7 vs. 2.7×10^8) of bacteria. When we extended Met treatment to 7 days, the WT mice also were infected (data not shown).

Perhaps it is expected that GPx1 and GPx2 play a important role in defending bacterial infection, because expression of both *Gpx1* and *Gpx2* is modulated by selenium (Se) [5] and Se-deficient mice were susceptible to food borne pathogens such as *Listeria monocytogenes* and *Citrobacter rodentium* [40–42]. Nevertheless, this is the first report to identify GPx1 and GPx2 as two major selenoproteins that protect gut from bacteria-induced colitis. Se deficiency-induced loss of GPx1 activity increases the susceptibility of humans and mice to coxsackievurus-induced cardiomyopathy [43]. Although the Gpx2 mRNA level is rather resistant to Se modulation, GPX2 protein expression is sensitive to Se deprivation, similarly to GPX1 [5, 19].

The more severe Salmonella-induced colitis in Gpx1-KO mice as compared to Gpx2-KO mice is likely due to the ubiquitous expression of the *Gpx1* gene. The *Gpx1* is expressed evenly in gut mucosal epithelium and lamina propria, while *Gpx2* is expressed specifically in the epithelium and highly in the crypt [19, 44]. GPX1-deficiency augmented lipopolysaccharide-induced *CD14* gene expression in human and mouse endothelial cells to induce expression of proinflammatory cytokines and adhesion molecules [24] [45]. CD14 is a glycoprotein highly expressed on the surface of myeloid cells [45]. Thus, S. Tm-infected *Gdac1*[B6] Gpx1-KO colon will have more inflammatory cells, which highly express *Nod2, Tnf, Nox2, Cd14, Cox2, Il1b* and *Nlrp3* genes.

We suspected that Gpx2-KO mice would be sensitive to bacterial infection because gut microbes are essential for causing ileocolitis in the Gpx1/2-DKO mice [18] and Se-deficient Gpx2-KO, but not Gpx1-KO, mice develop spontaneous colitis [5]. Here, we demonstrated that Gpx2-KO mice are susceptible to *S*. Tm-induced colitis compared to WT mice based on cecal pathology and Gdac1[B6] Gpx2-KO colon has lower villin mRNA levels compared to WT mouse colon. The mild elevation of inflammatory gene mRNA levels in the Gpx2-KO colon indicates that Gpx2-KO mice lack the strong inflammatory responses involving myeloid cells. We suspect that the excessive epithelial cell death in Gpx2-KO intestine makes them vulnerable to infection. Because *S*. Tm invasion of intestinal epithelial cells activates p53 and promotes apoptosis [46, 47], the additional stress in epithelial cells of Gpx2-KO intestine can lead to inflammation [48].

Since GPX2 modulates epithelial apoptosis, which can lead to inflammation when perturbed, we suspect the *Gdac1* gene(s) must modify the same pathway. DUOX2 is a prime candidate of a *Gdac1* gene, because 1) DUOX2 produces H_2O_2, a substrate for GPX1 and GPX2; 2) both Gpx2 and Duox2 are induced in S. Tm-induced colitis; 3) DUOX plays an

essential role in fending off ingested microbes [49, 50]; 4) DUOX2 has been identified as a binding partner of NOD2 and functions as an effecter of NOD2 activation [51]; and 5) there are three nonsynonymous single nucleotide polymorphisms between the B6 and 129 *Duox2* alleles [2], suggesting that these two alleles have different H_2O_2-producing activities. It is unclear why the *Gdac1B6* allele has opposite effects on spontaneous and pathogen-induced colitis. We suspect that stronger DUOX2129 activity than DUOX2B6 in the *Gdac1B6* locus (Leto, unpublished) is more effective at eliminating pathogens; however without abundant invading pathogens, the weaker DUOX2B6 provides sufficient oxidants to carry out signaling for infection-associated cell survival and wound healing [52, 53].

In this study, we used *villin* normalize epithelium-specific gene expression levels when comparing inflamed and normal intestine. Villin is a 92.5 kDa, actin-binding, cytoskeletal protein, which is located in intestinal microvilli to mediate cytoskeletal reorganization and has been well recognized as a marker for differentiated intestinal epithelial cells [54]. Although villin protein is highly dynamic, which is activated by epidermal growth factor to regulate actin assembly and cell migration, its mRNA levels remain constitutive [20]. Others have shown that decreased *villin* gene expression in the intestine is positively correlated with other epithelium-specific genes such as sucrose isomaltase expressed in differentiated enterocytes and α-defensin-5 and -6, defensin beta-1 as well as peptide YY in Paneth cell when comparing the normal and inflamed tissues of IBD patients [55–57]. Since we found villin mRNA levels are inversely correlated with pathology scores, and the severely inflamed intestine has lost epithelial cells, this is in complete agreement to others' idea to use villin gene expression levels as an indicator for inflammatory state reflecting loss of epithelial cells [55].

In summary, we have demonstrated that *Gdac1B6* alleviates colitis phenotypes in mice without severe deficiency of GPX in the absence of infectious agents. The *Gdac1* locus has an opposite effect on *S*. Tm-induced colitis, possibly due to a stronger anti-bacterial activity provided by DUOX2129, a *Gdac1* gene. We also illustrated that GPX1 and GPX2 singly protect mice from *S*. Tm infection. This provides the first evidence to demonstrate the importance of GPX1 and GPX2 in protecting intestine from bacterial infection.

Supplementary Material

Refer to Web version on PubMed Central for supplementary material.

Acknowledgments

REFERENCES

1. Esworthy RS, Kim BW, Larson GP, Yip ML, Smith DD, Li M, Chu FF. Colitis locus on chromosome 2 impacting the severity of early-onset disease in mice deficient in GPX1 and GPX2. Inflamm Bowel Dis. 2011; 17:1373–1386. [PubMed: 20872835]

2. Esworthy RS, Kim BW, Rivas GE, Leto TL, Doroshow JH, Chu FF. Analysis of candidate colitis genes in the gdac1 locus of mice deficient in glutathione peroxidase-1 and -2. PloS one. 2012; 7:e44262. [PubMed: 22970191]

3. Jostins L, Ripke S, Weersma RK, Duerr RH, McGovern DP, Hui KY, Lee JC, Schumm LP, Sharma Y, Anderson CA, Essers J, Mitrovic M, Ning K, Cleynen I, Theatre E, Spain SL, Raychaudhuri S, Goyette P, Wei Z, Abraham C, Achkar JP, Ahmad T, Amininejad L, Ananthakrishnan AN,

Andersen V, Andrews JM, Baidoo L, Balschun T, Bampton PA, Bitton A, Boucher G, Brand S, Buning C, Cohain A, Cichon S, D'Amato M, De Jong D, Devaney KL, Dubinsky M, Edwards C, Ellinghaus D, Ferguson LR, Franchimont D, Fransen K, Gearry R, Georges M, Gieger C, Glas J, Haritunians T, Hart A, Hawkey C, Hedl M, Hu X, Karlsen TH, Kupcinskas L, Kugathasan S, Latiano A, Laukens D, Lawrance IC, Lees CW, Louis E, Mahy G, Mansfield J, Morgan AR, Mowat C, Newman W, Palmieri O, Ponsioen CY, Potocnik U, Prescott NJ, Regueiro M, Rotter JI, Russell RK, Sanderson JD, Sans M, Satsangi J, Schreiber S, Simms LA, Sventoraityte J, Targan SR, Taylor KD, Tremelling M, Verspaget HW, De Vos M, Wijmenga C, Wilson DC, Winkelmann J, Xavier RJ, Zeissig S, Zhang B, Zhang CK, Zhao H, Silverberg MS, Annese V, Hakonarson H, Brant SR, Radford-Smith G, Mathew CG, Rioux JD, Schadt EE, Daly MJ, Franke A, Parkes M, Vermeire S, Barrett JC, Cho JH. Host-microbe interactions have shaped the genetic architecture of inflammatory bowel disease. Nature. 2012; 491:119–124. [PubMed: 23128233]

4. Dumitrescu AM, Di Cosmo C, Liao XH, Weiss RE, Refetoff S. The syndrome of inherited partial SBP2 deficiency in humans. Antioxid Redox Signal. 2010; 12:905–920. [PubMed: 19769464]

5. Esworthy RS, Yang L, Frankel PH, Chu FF. Epithelium-specific glutathione peroxidase, Gpx2, is involved in the prevention of intestinal inflammation in selenium-deficient mice. J Nutr. 2005; 135:740–745. [PubMed: 15795427]

6. Esworthy RS, Smith DD, Chu FF. A Strong Impact of Genetic Background on Gut Microflora in Mice. Int J Inflam. 2010; 2010:986046. [PubMed: 20976020]

7. Couturier-Maillard A, Secher T, Rehman A, Normand S, De Arcangelis A, Haesler R, Huot L, Grandjean T, Bressenot A, Delanoye-Crespin A, Gaillot O, Schreiber S, Lemoine Y, Ryffel B, Hot D, Nunez G, Chen G, Rosenstiel P, Chamaillard M. NOD2-mediated dysbiosis predisposes mice to transmissible colitis and colorectal cancer. J Clin Invest. 2013; 123:700–711. [PubMed: 23281400]

8. Ashida H, Ogawa M, Kim M, Mimuro H, Sasakawa C. Bacteria and host interactions in the gut epithelial barrier. Nat Chem Biol. 2012; 8:36–45. [PubMed: 22173358]

9. Gallois A, Klein JR, Allen LA, Jones BD, Nauseef WM. Salmonella pathogenicity island 2-encoded type III secretion system mediates exclusion of NADPH oxidase assembly from the phagosomal membrane. J Immunol. 2001; 166:5741–5748. [PubMed: 11313417]

10. Dandekar T, Astrid F, Jasmin P, Hensel M. Salmonella enterica: a surprisingly well-adapted intracellular lifestyle. Front Microbiol. 2012; 3:164. [PubMed: 22563326]

11. Stecher B, Robbiani R, Walker AW, Westendorf AM, Barthel M, Kremer M, Chaffron S, Macpherson AJ, Buer J, Parkhill J, Dougan G, von Mering C, Hardt WD. Salmonella enterica serovar typhimurium exploits inflammation to compete with the intestinal microbiota. PLoS Biol. 2007; 5:2177–2189. [PubMed: 17760501]

12. Ferreira RB, Gill N, Willing BP, Antunes LC, Russell SL, Croxen MA, Finlay BB. The intestinal microbiota plays a role in Salmonella-induced colitis independent of pathogen colonization. PLoS one. 2011; 6:e20338. [PubMed: 21633507]

13. Beck MA, Levander OA, Handy J. Selenium deficiency and viral infection. J Nutr. 2003; 133:1463S–1467S. [PubMed: 12730444]

14. Keestra AM, Winter MG, Klein-Douwel D, Xavier MN, Winter SE, Kim A, Tsolis RM, Baumler AJ. A Salmonella virulence factor activates the NOD1/NOD2 signaling pathway. MBio. 2011; 2

15. Wlodarska M, Willing B, Keeney KM, Menendez A, Bergstrom KS, Gill N, Russell SL, Vallance BA, Finlay BB. Antibiotic treatment alters the colonic mucus layer and predisposes the host to exacerbated Citrobacter rodentium-induced colitis. Infect Immun. 2011; 79:1536–1545. [PubMed: 21321077]

16. Savage DC, Dubos R, Schaedler RW. The gastrointestinal epithelium and its autochthonous bacterial flora. J Exp Med. 1968; 127:67–76. [PubMed: 4169441]

17. Lu P, Burger-van Paassen N, van der Sluis M, Witte-Bouma J, Kerckaert JP, van Goudoever JB, Van Seuningen I, Renes IB. Colonic gene expression patterns of mucin muc2 knockout mice reveal various phases in colitis development. Inflamm Bowel Dis. 2011

18. Chu FF, Esworthy RS, Chu PG, Longmate JA, Huycke MM, Wilczynski S, Doroshow JH. Bacteria-induced intestinal cancer in mice with disrupted Gpx1 and Gpx2 genes. Cancer Res. 2004; 64:962–968. [PubMed: 14871826]

19. Florian S, Krehl S, Loewinger M, Kipp A, Banning A, Esworthy S, Chu FF, Brigelius-Flohe R. Loss of GPx2 increases apoptosis, mitosis, and GPx1 expression in the intestine of mice. Free Radic Biol Med. 2010; 49:1694–1702. [PubMed: 20828612]

20. Khurana S, George SP. Regulation of cell structure and function by actin-binding proteins: villin's perspective. FEBS Lett. 2008; 582:2128–2139. [PubMed: 18307996]

21. Ogura Y, Inohara N, Benito A, Chen FF, Yamaoka S, Nunez G. Nod2, a Nod1/Apaf-1 family member that is restricted to monocytes and activates NF-kappaB. J. Biol. Chem. 2001; 276:4812–4818. [PubMed: 11087742]

22. Vazquez-Torres A, Xu Y, Jones-Carson J, Holden DW, Lucia SM, Dinauer MC, Mastroeni P, Fang FC. Salmonella pathogenicity island 2-dependent evasion of the phagocyte NADPH oxidase. Science. 2000; 287:1655–1658.. [PubMed: 10698741]

23. Rada B, Leto TL. Oxidative innate immune defenses by Nox/Duox family NADPH oxidases. Contrib Microbiol. 2008; 15:164–187. [PubMed: 18511861]

24. Lubos E, Mahoney CE, Leopold JA, Zhang YY, Loscalzo J, Handy DE. Glutathione peroxidase-1 modulates lipopolysaccharide-induced adhesion molecule expression in endothelial cells by altering CD14 expression. Faseb J. 2010; 24:2525–2532. [PubMed: 20219985]

25. Baumann CL, Aspalter IM, Sharif O, Pichlmair A, Bluml S, Grebien F, Bruckner M, Pasierbek P, Aumayr K, Planyavsky M, Bennett KL, Colinge J, Knapp S, Superti-Furga G. CD14 is a coreceptor of Toll-like receptors 7 and 9. J Exp Med. 2010; 207:2689–2701. [PubMed: 21078886]

26. Frolova L, Drastich P, Rossmann P, Klimesova K, Tlaskalova-Hogenova H. Expression of Toll-like receptor 2 (TLR2), TLR4, and CD14 in biopsy samples of patients with inflammatory bowel diseases: upregulated expression of TLR2 in terminal ileum of patients with ulcerative colitis. J Histochem Cytochem. 2008; 56:267–274. [PubMed: 18040078]

27. Haworth R, Oakley K, McCormack N, Pilling A. Differential expression of COX-1 and COX-2 in the gastrointestinal tract of the rat. Toxicol Pathol. 2005; 33:239–245. [PubMed: 15902967]

28. Ishikawa TO, Oshima M, Herschman HR. Cox-2 deletion in myeloid and endothelial cells, but not in epithelial cells, exacerbates murine colitis. Carcinogenesis. 2011; 32:417–426. [PubMed: 21156970]

29. Schoenborn JR, Wilson CB. Regulation of interferon-gamma during innate and adaptive immune responses. Advances in immunology. 2007; 96:41–101. [PubMed: 17981204]

30. Bernink JH, Peters CP, Munneke M, te Velde AA, Meijer SL, Weijer K, Hreggvidsdottir HS, Heinsbroek SE, Legrand N, Buskens CJ, Bemelman WA, Mjosberg JM, Spits H. Human type 1 innate lymphoid cells accumulate in inflamed mucosal tissues. Nat Immunol. 2013; 14:221–229. [PubMed: 23334791]

31. Jabaut J, Ather JL, Taracanova A, Poynter ME, Ckless K. Mitochondria-targeted drugs enhance Nlrp3 inflammasome-dependent IL-1beta secretion in association with alterations in cellular redox and energy status. Free Radic Biol Med. 2013; 60C:233–245. [PubMed: 23376234]

32. Schroder K, Tschopp J. The inflammasomes. Cell. 2010; 140:821–832. [PubMed: 20303873]

33. Anderson JP, Mueller JL, Rosengren S, Boyle DL, Schaner P, Cannon SB, Goodyear CS, Hoffman HM. Structural, expression, and evolutionary analysis of mouse CIAS1. Gene. 2004; 338:25–34. [PubMed: 15302403]

34. Rodenburg W, Keijer J, Kramer E, Roosing S, Vink C, Katan MB, van der Meer R, Bovee-Oudenhoven IM. Salmonella induces prominent gene expression in the rat colon. BMC Microbiol. 2007; 7:84. [PubMed: 17850650]

35. Geiszt M, Witta J, Baffi J, Lekstrom K, Leto TL. Dual oxidases represent novel hydrogen peroxide sources supporting mucosal surface host defense. FASEB J. 2003; 17:1502–1504. [PubMed: 12824283]

36. Esworthy RS, Mann JR, Sam M, Chu FF. Low glutathione peroxidase activity in Gpx1 knockout mice protects jejunum crypts from gamma-irradiation damage. Am J Physiol Gastrointest Liver Physiol. 2000; 279:G426–G436. [PubMed: 10915653]

37. Park KJ, Lee CH, Kim A, Jeong KJ, Kim CH, Kim YS. Death receptors 4 and 5 activate Nox1 NADPH oxidase through riboflavin kinase to induce reactive oxygen species-mediated apoptotic cell death. J. Biol. Chem. 2012; 287:3313–3325. [PubMed: 22158615]

38. Szanto I, Rubbia-Brandt L, Kiss P, Steger K, Banfi B, Kovari E, Herrmann F, Hadengue A, Krause KH. Expression of NOX1, a superoxide-generating NADPH oxidase, in colon cancer and inflammatory bowel disease. J Pathol. 2005; 207:164–176. [PubMed: 16086438]

39. Romanoski CE, Che N, Yin F, Mai N, Pouldar D, Civelek M, Pan C, Lee S, Vakili L, Yang WP, Kayne P, Mungrue IN, Araujo JA, Berliner JA, Lusis AJ. Network for activation of human endothelial cells by oxidized phospholipids: a critical role of heme oxygenase 1. Circ Res. 2011; 109:e27–e41. [PubMed: 21737788]

40. Wang C, Wang H, Luo J, Hu Y, Wei L, Duan M, He H. Selenium deficiency impairs host innate immune response and induces susceptibility to Listeria monocytogenes infection. BMC Immunol. 2009; 10:55. [PubMed: 19852827]

41. Smith AD, Botero S, Shea-Donohue T, Urban JF Jr. The pathogenicity of an enteric Citrobacter rodentium Infection is enhanced by deficiencies in the antioxidants selenium and vitamin E. Infect Immun. 2011; 79:1471–1478. [PubMed: 21245271]

42. Smith AD, Cheung L, Botero S. Long-term selenium deficiency increases the pathogenicity of a Citrobacter rodentium infection in mice. Biol Trace Elem Res. 2011; 144:965–982. [PubMed: 21584659]

43. Beck MA, Esworthy RS, Ho YS, Chu FF. Glutathione peroxidase protects mice from viral-induced myocarditis. Faseb J. 1998; 12:1143–1149. [PubMed: 9737717]

44. Chu FF, Esworthy RS. The expression of an intestinal form of glutathione peroxidase (GSHPx-GI) in rat intestinal epithelium. Arch Biochem Biophys. 1995; 323:288–294. [PubMed: 7487090]

45. Lubos E, Kelly NJ, Oldebeken SR, Leopold JA, Zhang YY, Loscalzo J, Handy DE. Glutathione Peroxidase-1 (GPx-1) deficiency augments pro-inflammatory cytokine-induced redox signaling and human endothelial cell activation. J. Biol. Chem. 2011

46. Wu S, Ye Z, Liu X, Zhao Y, Xia Y, Steiner A, Petrof EO, Claud EC, Sun J. Salmonella typhimurium infection increases p53 acetylation in intestinal epithelial cells. Am J Physiol Gastrointest Liver Physiol. 2010; 298:G784–G794. [PubMed: 20224008]

47. Martinez Rodriguez NR, Eloi MD, Huynh A, Dominguez T, Lam AH, Carcamo-Molina D, Naser Z, Desharnais R, Salzman NH, Porter E. Expansion of Paneth cell population in response to enteric Salmonella enterica serovar Typhimurium infection. Infect Immun. 2012; 80:266–275. [PubMed: 22006567]

48. Ashida H, Mimuro H, Ogawa M, Kobayashi T, Sanada T, Kim M, Sasakawa C. Cell death and infection: a double-edged sword for host and pathogen survival. J. Cell Biol. 2011; 195:931–942. [PubMed: 22123830]

49. Buchon N, Broderick NA, Poidevin M, Pradervand S, Lemaitre B. Drosophila intestinal response to bacterial infection: activation of host defense and stem cell proliferation. Cell Host Microbe. 2009; 5:200–211. [PubMed: 19218090]

50. Flores MV, Crawford KC, Pullin LM, Hall CJ, Crosier KE, Crosier PS. Dual oxidase in the intestinal epithelium of zebrafish larvae has anti-bacterial properties. Biochem Biophys Res Commun. 2010; 400:164–168. [PubMed: 20709024]

51. Lipinski S, Till A, Sina C, Arlt A, Grasberger H, Schreiber S, Rosenstiel P. DUOX2-derived reactive oxygen species are effectors of NOD2-mediated antibacterial responses. J Cell Sci. 2009; 122:3522–3530. [PubMed: 19759286]

52. Yu M, Lam J, Rada B, Leto TL, Levine SJ. Double-stranded RNA induces shedding of the 34-kDa soluble TNFR1 from human airway epithelial cells via TLR3-TRIF-RIP1-dependent signaling: roles for dual oxidase 2- and caspase-dependent pathways. J Immunol. 2011; 186:1180–1188. [PubMed: 21148036]

53. Niethammer P, Grabher C, Look AT, Mitchison TJ. A tissue-scale gradient of hydrogen peroxide mediates rapid wound detection in zebrafish. Nature. 2009; 459:996–999. [PubMed: 19494811]

54. Cheung R, Kelly J, Macleod RJ. Regulation of villin by wnt5a/ror2 signaling in human intestinal cells. Frontiers in physiology. 2011; 2:58. [PubMed: 21949508]

55. Simms LA, Doecke JD, Walsh MD, Huang N, Fowler EV, Radford-Smith GL. Reduced alpha-defensin expression is associated with inflammation and not NOD2 mutation status in ileal Crohn's disease. Gut. 2008; 57:903–910. [PubMed: 18305068]

56. Arijs I, De Hertogh G, Lemaire K, Quintens R, Van Lommel L, Van Steen K, Leemans P, Cleynen I, Van Assche G, Vermeire S, Geboes K, Schuit F, Rutgeerts P. Mucosal gene expression of antimicrobial peptides in inflammatory bowel disease before and after first infliximab treatment. PloS one. 2009; 4:e7984. [PubMed: 19956723]

57. Nijmeijer RM, Gadaleta RM, van Mil SW, van Bodegraven AA, Crusius JB, Dijkstra G, Hommes DW, de Jong DJ, Stokkers PC, Verspaget HW, Weersma RK, van der Woude CJ, Stapelbroek JM, Schipper ME, Wijmenga C, van Erpecum KJ, Oldenburg B, Dutch Initiative on Crohn C. Farnesoid X receptor (FXR) activation and FXR genetic variation in inflammatory bowel disease. PloS one. 2011; 6:e23745. [PubMed: 21887309]

Highlights

- The *Gdac1* locus modifies colitis severity and was identified by comparing the B6 and 129 Gpx1/2-DKO mice.

- Congenic 129-*Gdac1*^{B6} Gpx1-KO or Gpx2-KO mice have attenuated colitis in the absence of pathogens compared to 129 strain mice.

- However, 129-*Gdac1*^{B6} Gpx1-KO mice have stronger inflammatory responses to Salmonella-induced colitis than 129 strain mice.

- *Gdac1* has an opposite effect on spontaneous versus bacteria-associated colitis.

- GPx1 and GPx2 individually protect mice against Salmonella-induced colitis.
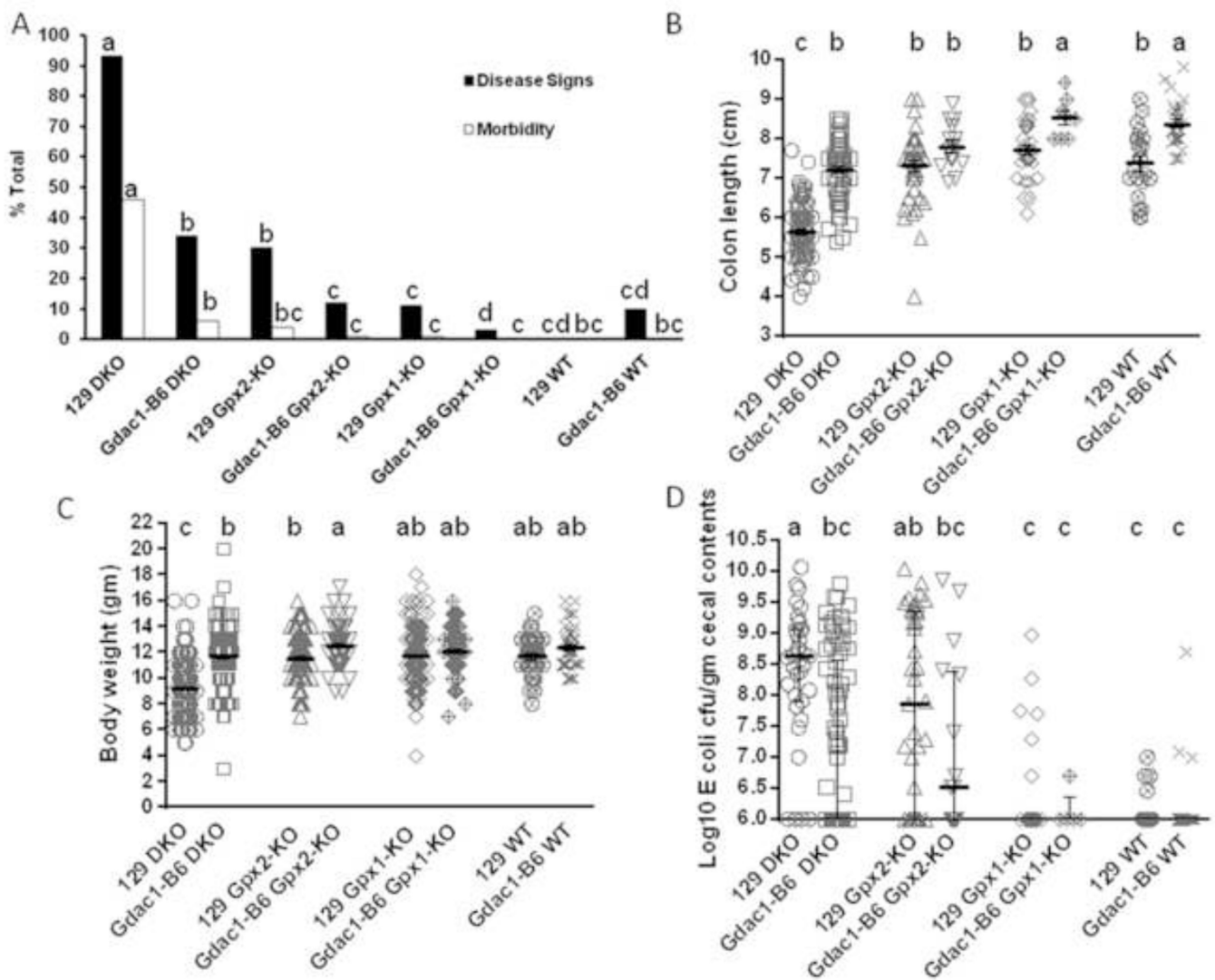
Figure 1.

Impact of the *Gdac1* locus on spontaneous colitis in 129 strain mice with and without Gpx1 and Gpx2 deficiency.

A. The percentage of mice that showed colitis disease signs and morbidity at 22 days of age. The *Gdac1* effect was analyzed in four groups of mice: Gpx1−/−Gpx2−/− (DKO), Gpx1+/−Gpx2−/− (Gpx2-KO), Gpx1−/−Gpx2+/− (Gpx1-KO) and wild-type (WT) of 129 background that carried either the *Gdac1*[129] (129) or *Gdac1*[B6] locus (*Gdac1*-B6). The percentages of mice in each group that had disease signs (solid bar) or morbidity (open bar) were analyzed separately. N = 574 129 DKO, 156 *Gdac1*[B6] DKO, 315 129 Gpx2-KO, 80 *Gdac1*[B6] Gpx2-KO, 352 129 Gpx1-KO, 114 *Gdac1*[B6] Gpx1-KO, 30 129 WT and 10 *Gdac1*[B6] WT. Groups with significantly different disease incidence are indicated by different letters, where a>b>c>d. Groups that share a letter are not statistically different (i.e., bc is not different from b or c, and cd is not different from c or d).

B. Scatter dot plot of colon length of mice at 22 days of age. The same genotypes of mice were used as in A. The gray horizontal lines are mean ± SEM. N= 106 129 DKO, 69 *Gdac1*[B6] DKO, 46 129 Gpx2-KO, 15 *Gdac1*[B6] Gpx2-KO, 36 129 Gpx1-KO, 8 *Gdac1*[B6]

Gpx1-KO, 22 129 WT and 29 *Gdac1*^{B6} WT. Groups with significantly different means are indicated by different letters, where a>b>c. C.

Scatter dot plot of mouse body weight of mice at 22 days of age. The gray lines with error bars indicate mean ± SEM. N= 339 129 DKO, 147 *Gdac1*^{B6} DKO, 193 129 Gpx2-KO, 72 *Gdac1*^{B6} Gpx2-KO, 293 129 Gpx1-KO, 97 *Gdac1*^{B6} Gpx1-KO, 36 129 WT and 43 *Gdac1*^{B6} WT mice. Groups with significantly different means are indicated by different letters, where a>b>c. Groups that share a letter are not significantly different (i.e., ab is not different from a or b).

D. Scatter dot plot of mouse gut dysbiosis. Gdac1^{B6} DKO mice had significantly lower *E. coli* counts than did 129 DKO mice, while 129 Gpx2-KO mice had higher *E. coli* counts than did Gpx1-KO and WT mice. n = 35 129 DKO, 82 Gdac1^{B6} DKO, 41 129 Gpx2-KO, 16 *Gdac1*^{B6} Gpx2-KO, 38 129 Gpx1-KO, 5 *Gdac1*^{B6} Gpx1-KO, 25 129 WT and 29 *Gdac1*^{B6} WT mice. The gray horizontal lines with error bars indicate median ± interquartile range. Medians that differ are indicated by different letters, where a>b>c. Groups that share a letter are not statistically different (i.e., ab is not different from a or bc, and bc is not different from c).
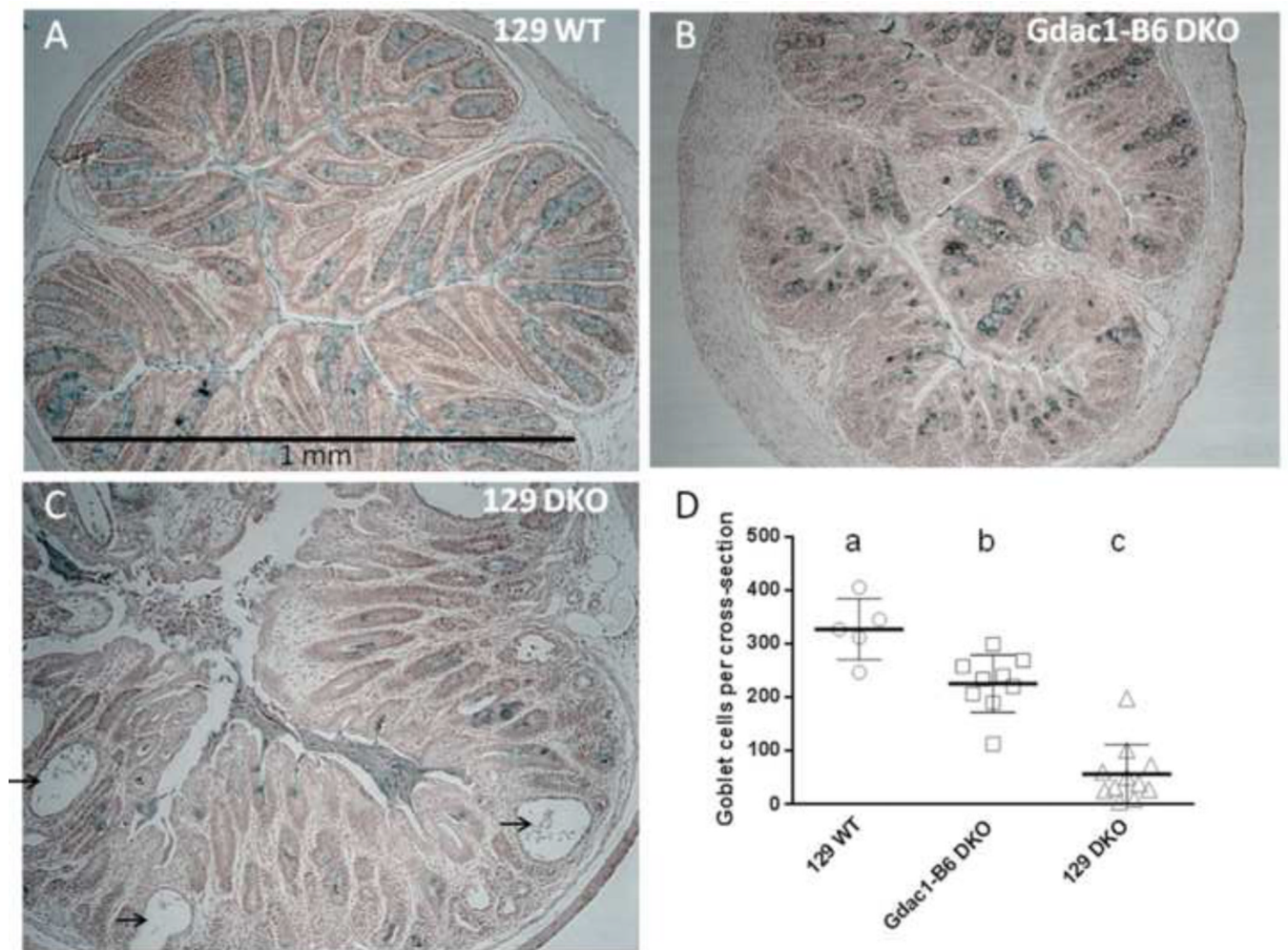
Figure 2.
The *Gdac1* locus modulates goblet cell number in the colon of DKO mice. Panels A-C are representative cross sections of mouse colon of 129 WT, Gdac1[B6] DKO and 129 DKO, respectively, stained with Alcian blue. Arrows point at exfoliated epithelial cells in postinflamed crypts. Panel D shows the total number of alcian blue-stained cells in each cross section from 5 129 WT, 9 Gdac1[B6] DKO and 11 129 DKO colon. The black horizontal lines with error bars indicate mean ± SEM.
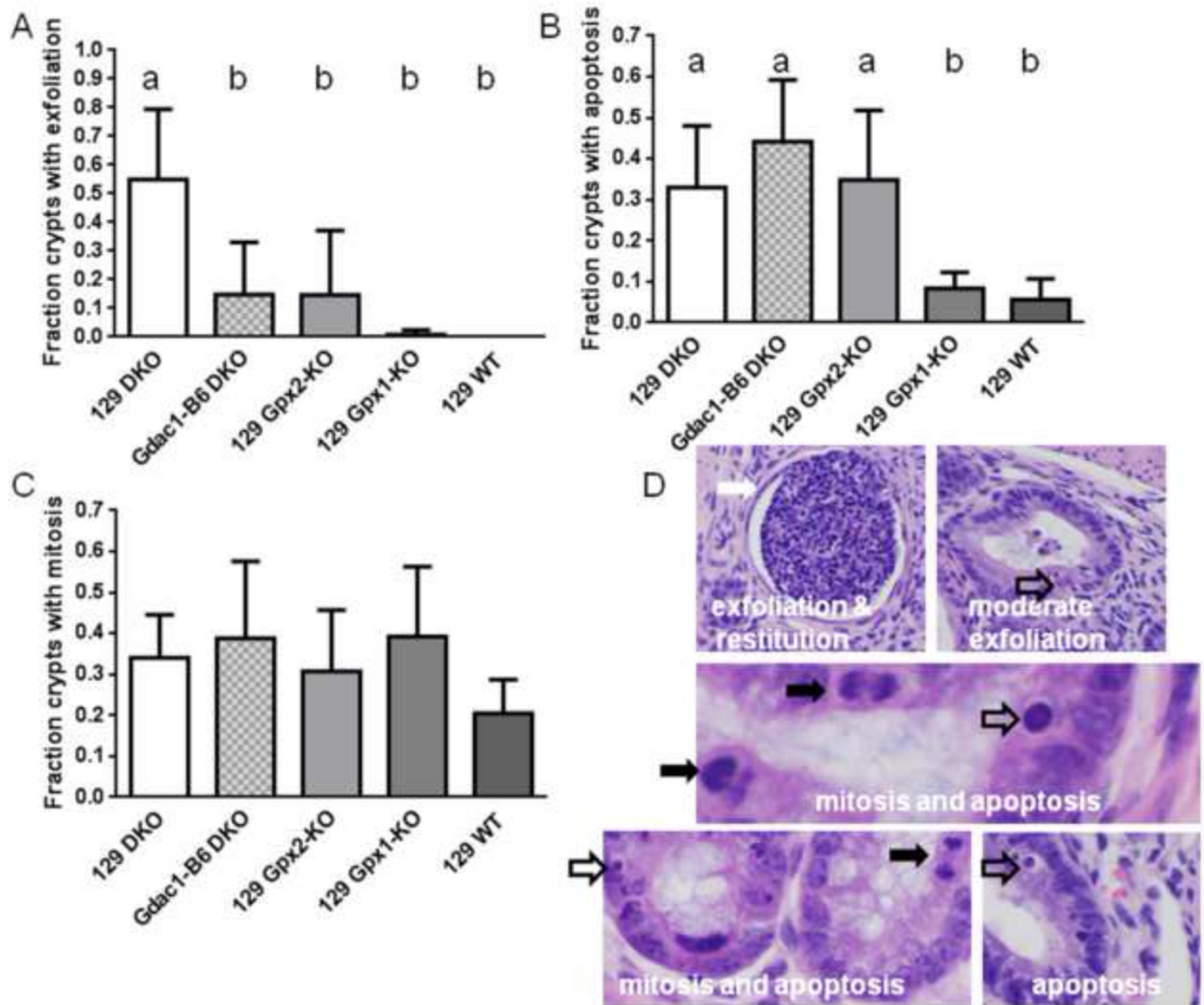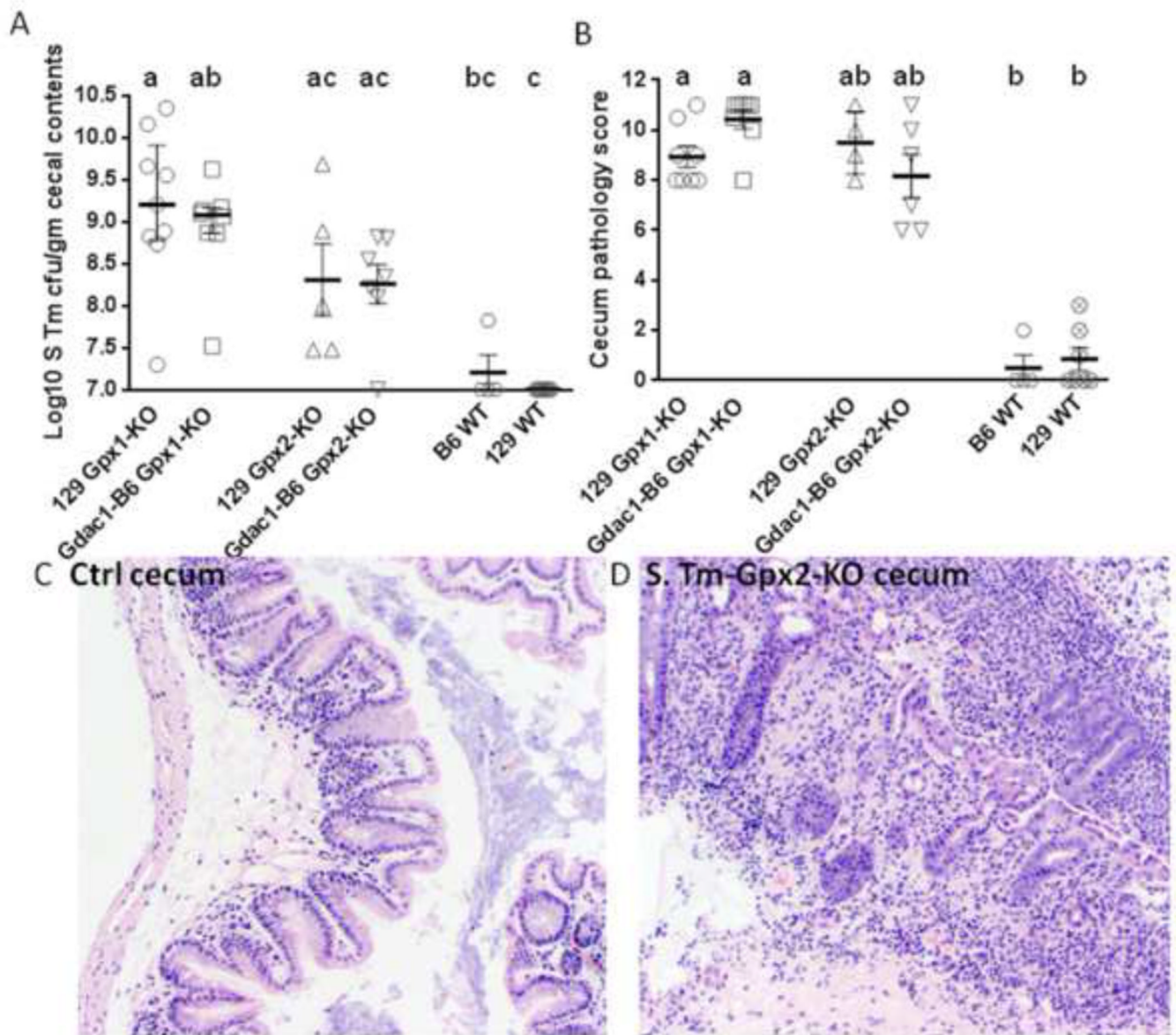
Figure 3.
The *Gdac1* locus modulates crypt exfoliation but not epithelial apoptosis or mitosis in the colon of DKO mice. Panel A shows that 55% of colon crypt in 129 DKO mice had exfoliated epithelial cells, while 15% and 15% of colon crypt in Gdac1[B6] DKO and 129 Gpx2-KO colon, respectively, had. 129 Gpx1-KO and WT mice did not have significant crypt epithelial cell exfoliation. n=124–199 crypts (5–10 mice). The groups that differ are indicated by different letters, where a>b. Panel B shows the fraction of crypts has at least one apoptotic cell; that is 0.33 in 129 DKO, 0.45 in Gdac1[B6] DKO, 0.36 in Gpx2-KO, 0.11 in Gpx1-KO and 0.06 in 129 WT colon crypt. n= 90–200 crypts (5–10 mice). The groups that differ are indicated by different letters, where a>b. Panel C shows the fraction of crypt has at least one mitotic cell; that is 0.34 in 129 DKO, 0.39 in Gdac1[B6] DKO, 0.31 in Gpx2-KO, 0.39 in Gpx1-KO and 0.21 in 129 WT colon crypt. n= 90–200 crypts (5–10 mice). Panel D shows H&E staining of 129 DKO colon crypts. The white arrow indicates restitution in response to loss of epithelium, the open arrows point at apoptotic cells and the black arrowheads point at mitotic cells. The top two photos show extreme (left) and mild

(right) exfoliation. The left photo shows restitution (flattening) of crypt epithelium in response to extreme cell loss, when the right photo shows near normal morphology.
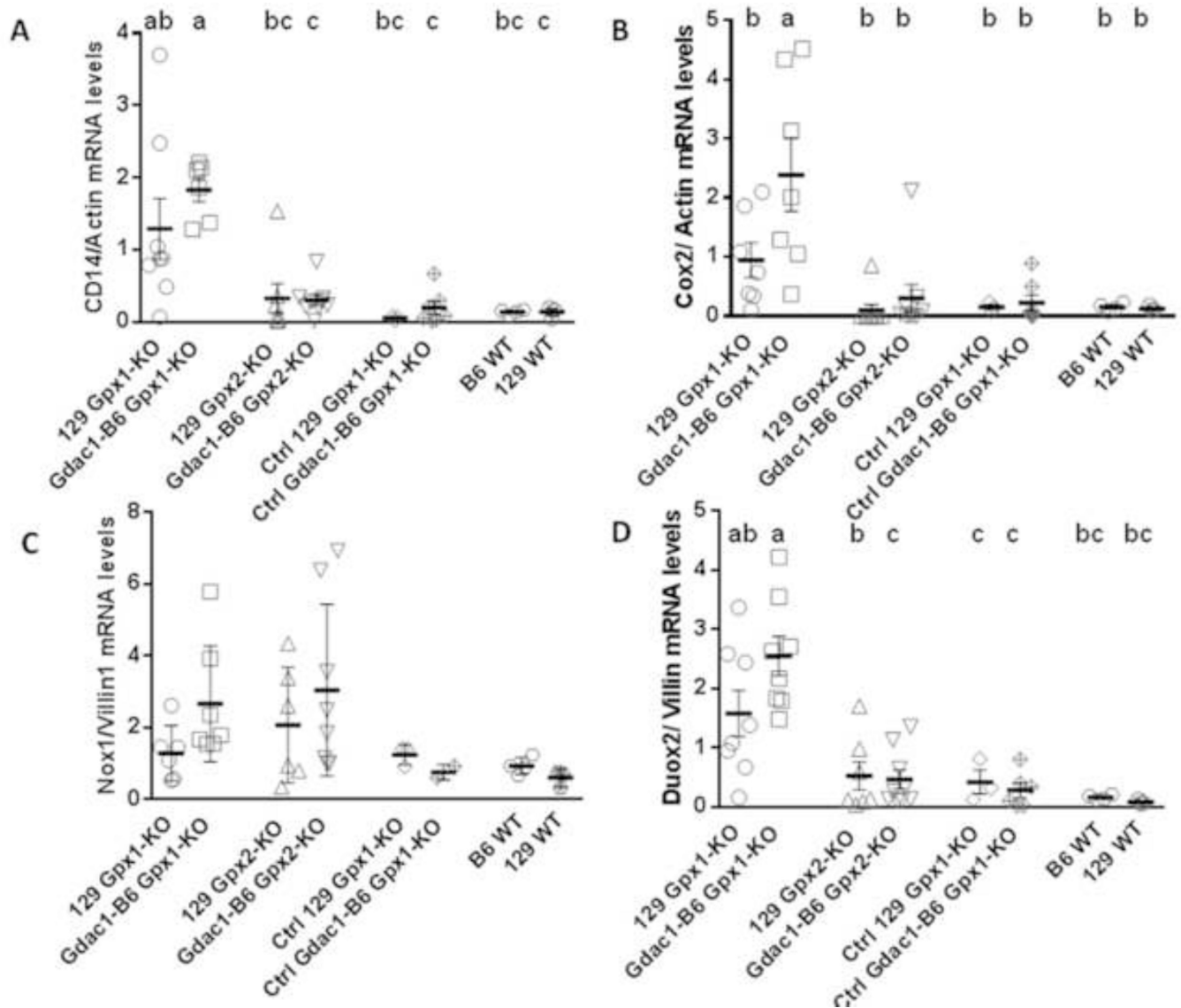
Figure 4.
GPx1 and GPx2, but not the *Gdac1* locus, protects mice from *S*. Tm-induced colitis. Panel A is a scatter dot plot of *S*. Tm colonization in the cecum of mice pretreated with metronidazole. Each symbol represents one mouse. The horizontal bars are median ± interquartile range. N = 9 129 GPx1-KO, 8 Gdac1-B6 GPx1-KO, 5 129 GPx2-KO, 7 Gdac1-B6 GPx2-KO, 4 WT B6 and 7 129 WT mice. Medians that differ are indicated by different letters, where a>b>c. Groups that share a letter are not a statistically different (i.e., ab is not different from a or b). Panel B shows a scatter dot plot of cecum pathology analyzed at 4 days post *S*. Tm inoculation. The horizontal lines are median ± interquartile range. N = 8 each of 129 GPx1-KO and Gdac1-B6 GPx1-KO, 5 129 GPx2-KO, 7 Gdac1-B6 GPx2-KO, 4 B6 WT and 7 129 WT mice. Medians that differ are indicated by different letters, where a>b. The control 10 129 Gpx1-KO and 6 Gpx2-KO mice had a median pathology score of 1 (range 0–7). Panels C and D are H&E stained cecum cross section from a non-infected and

S. Tm-infected 129 Gpx2-KO mouse, respectively. The *S*. Tm-infected cecum has many infiltrating cells and distorted glands.
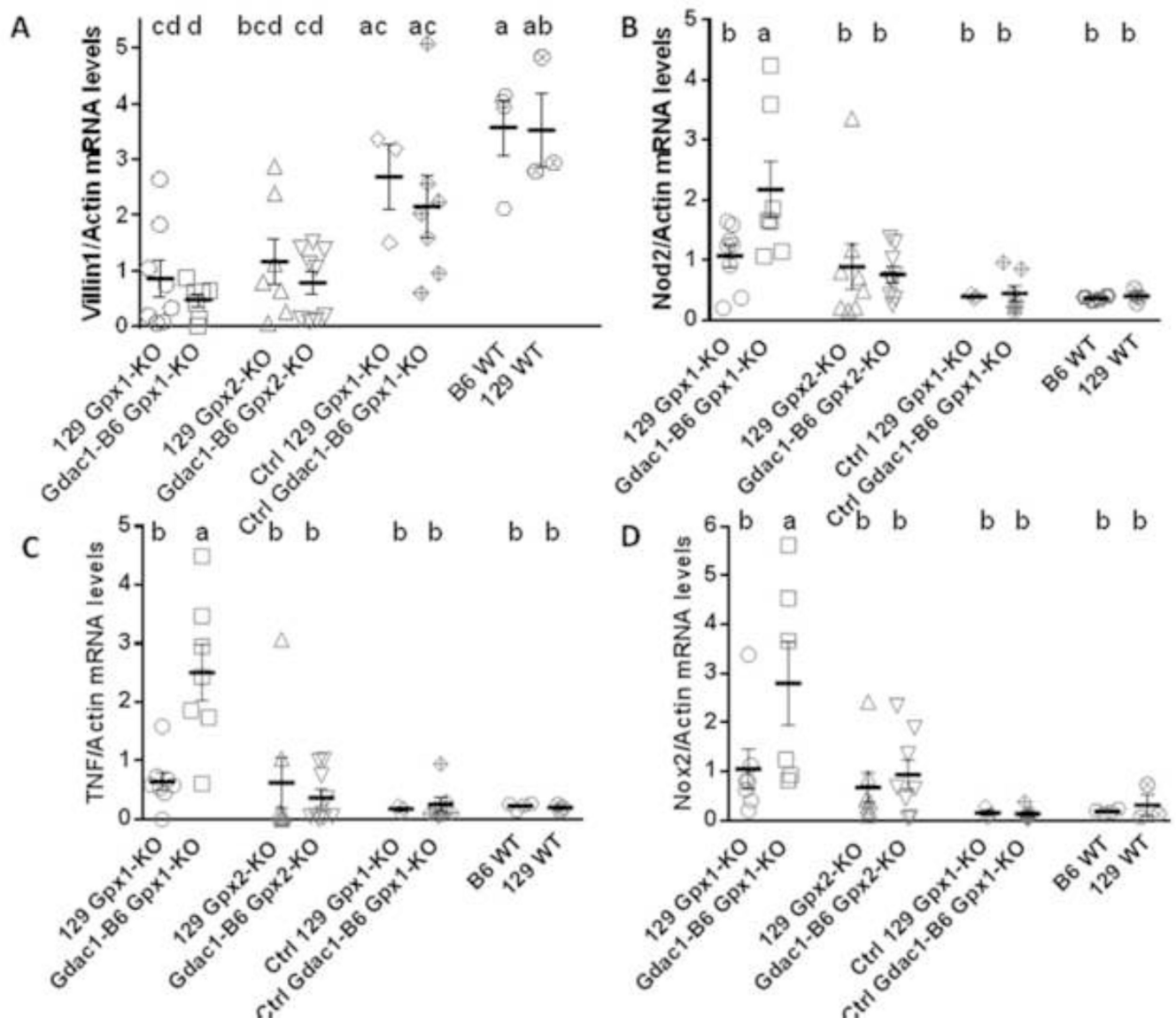
Figure 5.
Scatter dot plot of *villin* (A), Nod2 (B), Tnf (C) and Nox2 (D) mRNA levels in the cecum of mice after inoculation with *S*. Tm. Control (Ctrl) 129 GPx1-KO and congenic Gdac1[B6] GPx1-KO mice were either pre-treated with metronidazole (Met) without *S*. Tm inoculation or were inoculated with *S*. Tm without Met pretreatment. All mRNA was normalized to β-actin. The horizontal lines are mean ± SEM. N = 7–8 129 Gpx1-KO, 6–7 Gdac1-B6 Gpx1-KO, 7–8 129 Gpx2-KO, 8–9 Gdac1-B6 Gpx2-KO, 3 Ctrl 129 Gpx1-KO, 7 Ctrl Gdac1-B6 Gpx1-KO, 4 B6 WT and 3 129 WT mice for all mRNAs. Means that differ are indicated by different letters (where a>b>c). Groups share the same letter are not different (e.g cd is not different from d, bcd or ac).

Figure 6.
Scatter dot plots of *Cd14* (A), *Cox2* (B), *Nox1* (C) and *Duox2* (D) mRNA levels in mouse cecum. *Cd14* and *Cox2* mRNA expression were normalized against β-actin, while *Nox1* and *Duox2* mRNA levels were normalized against *villin*. The horizontal lines indicate mean ± SEM, each symbol indicates one mouse. n = 6–8 129 Gpx1-KO, 6–8 Gdac1-B6 Gpx1-KO, 6–9 129 Gpx2-KO, 8–9 Gdac1-B6 Gpx2-KO, 3 Ctrl 129 Gpx1-KO, 6–7 Ctrl Gdac1-B6 Gpx1-KO (except 2 for Nox1 mRNA), 4 B6 WT and 3 129 WT mice for all mRNAs. Means that differ are indicated by different letters, where a>b. Groups that share a letter are not different (i.e., ab is not different from a, b or bc).

Table 1

Real-time PCR primer sequences for mouse cDNA

Cd14	Forward 5'-CATTTGCATCCTCCTGGTTTCTGA-3'
	Reverse 5'-GAGTGAGTTTTCCCCTTCCGTGTG-3'
Chac1	Forward 5'-CTGTGGATTTTCGGGTACGG-3'
	Reverse 5'-CTCGGCCAGGCATCTTGTC-3'
Cox2	Forward 5'-TGTGACTGTACCCGGACTGG-3'
	Reverse 5'-TGCACATTGTAAGTAGGTGGAC-3'
Duox2	Forward 5'-TCACAACGGACGGCTTGCCC-3'
	Reverse 5'-CCCGGCCACTCCATTGCTGG-3'
Gpx2	Forward 5'-GAGGAACAACTACCCGGGACTA-3'
	Reverse 5'-ACCCCCAGGTCGGACATACT-3'
Ifn-γ	Forward 5'-ATGAACGCTACACACTGCATC-3'
	Reverse 5'-CCATCCTTTTGCCAGTTCCTC-3'
IL1β	Forward 5'-CTGCAGCTGGAGAGTGTGG-3'
	Reverse 5'-GGGGAACTCTGCAGACTCAA-3'
Nlrp3	Forward 5'-ATGGCTGTGTGGATCTTTGC-3'
	Reverse 5'-CACGTGTCATTCCACTCTGG-3'
Nod2	Forward 5'-CCTGGTACGTGCCCAAAGTAG -3'
	Reverse 5'-GCCAAGTAGAAAGCGGCAAA -3'
Nox1	Forward 5'-CTCCCTTTGCTTCCATCTTG-3'
	Reverse 5'-GCAAAGGCACCTGTCTCTCTA-3'
Nox2	Forward 5'-TGAGAGGTTGGTTCGGTTTT-3'
	Reverse 5'-GTTTTGAAAGGGTGGGTGAC-3'
Tnf	Forward 5'-CATCTTCTCAAAATTCGAGTGACAA-3'
	Reverse 5'-TGGGAGTAGACAAGGTACAACCC-3'
Villin	Forward 5'-TCAAAGGCTCTCTCAACATCAC-3'
	Reverse 5'-AGCAGTCACCATCGAAGAAGC-3'